Structure
Article

Crystal Structure of cGMP-Dependent Protein Kinase Reveals Novel Site of Interchain Communication

Brent W. Osborne,[1,7] Jian Wu,[2,7] Caitlin J. McFarland,[1] Christian K. Nickl,[1] Banumathi Sankaran,[3] Darren E. Casteel,[4] Virgil L. Woods, Jr.,[4] Alexandr P. Kornev,[2,6] Susan S. Taylor,[2,5,6] and Wolfgang R. Dostmann[1,*]
[1]Department of Pharmacology, College of Medicine, University of Vermont, Burlington, VT 05405, USA
[2]Department of Pharmacology, University of California San Diego, La Jolla, CA 92093, USA
[3]The Berkeley Center for Structural Biology, Lawrence Berkeley National Laboratory, Berkeley, CA 94720, USA
[4]Department of Medicine and Cancer Center
[5]Department of Chemistry and Biochemistry
[6]Howard Hughes Medical Institute
University of California, San Diego, La Jolla, CA 92093, USA
[7]These authors contributed equally to this work
*Correspondence: wolfgang.dostmann@uvm.edu
DOI 10.1016/j.str.2011.06.012

SUMMARY

The cGMP-dependent protein kinase (PKG) serves as an integral component of second messenger signaling in a number of biological contexts including cell differentiation, memory, and vasodilation. PKG is homodimeric and large conformational changes accompany cGMP binding. However, the structure of PKG and the molecular mechanisms associated with protomer communication following cGMP-induced activation remain unknown. Here, we report the 2.5 Å crystal structure of a regulatory domain construct (aa 78–355) containing both cGMP binding sites of PKG Iα. A distinct and segregated architecture with an extended central helix separates the two cGMP binding domains. Additionally, a previously uncharacterized helical domain (switch helix) promotes the formation of a hydrophobic interface between protomers. Mutational disruption of this interaction in full-length PKG implicates the switch helix as a critical site of dimer communication in PKG biology. These results offer new structural insight into the mechanism of allosteric PKG activation.

INTRODUCTION

As key members of the AGC family of protein kinases, all mammalian PKG isoforms (Iα, Iβ, II) share a similar domain configuration (Figure 1A). At their N termini, coiled coils promote a parallel homodimeric configuration, followed by an autoinhibitory domain (AI) and two tandem cyclic nucleotide (cNT) binding sites, which cooperatively regulate C-terminal catalytic activity (for review, see Francis and Corbin, 1994; Hofmann et al., 2009; Pfeifer et al., 1999; Vaandrager et al., 2005). The current model of PKG Iα holoenzyme assembly and mechanism of activation stresses the importance of the AI domain (aa 64–78) within the N-terminal region (Heil et al., 1987; Wolfe et al., 1989). This flexible hinge segment has a pseudo-substrate sequence and is believed to autoinhibit the C-terminal catalytic center in the enzyme's dormant state (Kennelly and Krebs, 1991; Landgraf and Hofmann, 1989; Ruth et al., 1991). Autophosphorylation at various N-terminal residues appears to weaken this intramolecular inhibitory interaction; however, only cGMP binding to both the A- and B-domains induces the conformational change necessary for full kinase activity (Aitken et al., 1984; Chu et al., 1997; Francis et al., 2002). Although it is believed that the dimer stays intact upon cGMP-induced activation, the overall conformational change is substantial (Alverdi et al., 2008; Richie-Jannetta et al., 2006; Zhao et al., 1997). A significant molecular elongation centered about both the N-terminal dimerization domain (D/D) as well as the C-terminal catalytic domain accompanies cGMP-induced activation. It is at this level of allosteric modulation that underscores the most distinct difference between PKG and the cAMP-dependent protein kinase (PKA). While the regulatory and catalytic subunits of PKA dissociate upon cyclic nucleotide-induced activation (Gill and Garren, 1971), PKG harbors these components on the same polypeptide chain (Sandberg et al., 1989; Takio et al., 1984; Wernet et al., 1989). Another notable difference for all cyclic nucleotide kinases is their distinct structural order of high and low affinity cyclic nucleotide binding. For PKG I, the high affinity cyclic nucleotide sites are closer to the N termini, whereas for PKA I, PKA II and PKG II, the order of high and low nucleotide binding affinity sites is reversed (Reed et al., 1996). These structural differences suggest different means of activation by cyclic nucleotides and a comprehensive understanding of the mechanisms underlying cGMP-mediated PKG activation will invariantly require high-resolution biophysical studies.

To better understand the molecular details of PKG regulation, we solved the 2.5 Å crystal structure of a regulatory domain fragment of PKG Iα thought to be central for conveying allosteric modulation within the enzyme. The structure (amino acid residues 78–355) presents both tandem cGMP-binding domains

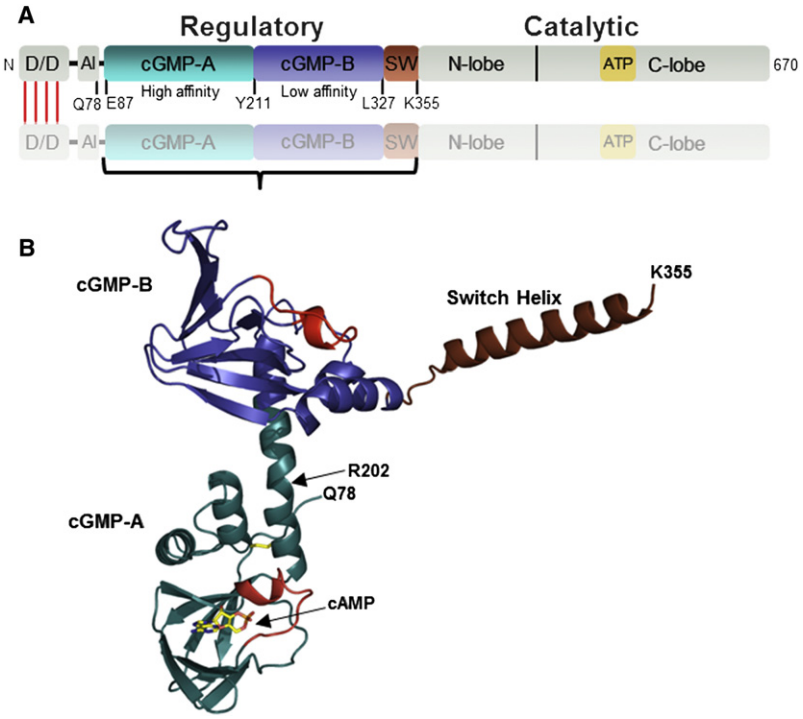

Figure 1. PKG Iα: Domain Organization and General Architecture of PKG$^{78\text{-}355}$

(A) D/D: docking and dimerization domain; AI: autoinhibitory domain; cGMP-A/B: cGMP binding sites A and B; SW: switch helix. Red bars at the N terminus indicate site of parallel homodimerization.

(B) Overall fold of PKG$^{78\text{-}355}$ (color coding same as above). See also Figure S1.

and identifies a novel helical subdomain (switch helix, SW) that follows cGMP-binding site B (Figure 1B). The A-site is cAMP-bound and confirms a previously suggested disulfide bond between Cys^{117} and Cys^{195}. The B-domain is not cNT-occupied, but rather stabilized by hydrophobic contacts with the SW from the other protein molecule in the asymmetric unit. This hydrophobic interaction highlights an unexpected natural interface, disruption of which alters the kinetic profile of full-length PKG Iα. Therefore, the PKG$^{78\text{-}355}$ structure expands our understanding of the landscape of PKG domain assembly and sheds new light on the molecular mechanism of holoenzyme formation and activation of PKG Iα.

RESULTS AND DISCUSSION

The greatest structural distinction between the two major cyclic nucleotide regulated protein kinases, PKA and PKG, is the fact that PKG maintains both its regulatory and catalytic elements on the same polypeptide chain (Gill et al., 1977), while PKA is divided into subunits (Gill and Garren, 1971). To better understand how these molecular differences contribute to the unique characteristics of each kinase, we crystallized the central portion of the regulatory domain of PKG Iα. While prokaryotic expression of PKG constructs containing the catalytic domain yields inactive, misfolded protein that is sequestered to inclusion bodies (Feil et al., 1993), previous attempts to crystallize full-length PKG from mammalian systems have been unsuccessful as well. This is in part due to conformational heterogeneity stemming from mixed phosphorylation states at the N terminus and a proteolytically exposed hinge at Arg^{77} (Aitken et al., 1984; Heil et al., 1987; Scholten et al., 2007). We hypothesized that exclusion of both the N-terminal D/D domain, as well as the C-terminal catalytic domain would give rise to a stable, monomeric fragment that is readily expressed in *Escherichia coli*. Multiple regulatory fragments were designed to encompass both tandem cGMP-binding domains (PKG$^{78\text{-}326}$, PKG$^{78\text{-}341}$, and PKG$^{78\text{-}355}$). The standard method for purification of recombinant PKG utilizes cyclic nucleotide affinity chromatography which saturates the allosteric binding sites through an elution with high concentrations of cNT (Dostmann et al., 1999). To prevent this artificial exposure of PKG protein to cNTs, PKG constructs were engineered with N-terminal hexa-histidine tags and purified using standard immobilized metal affinity chromatography (IMAC) methods. We made three PKG regulatory domain constructs (PKG$^{78\text{-}326}$, PKG$^{78\text{-}341}$, and PKG$^{78\text{-}355}$). Despite high yielding, stable expression of all three constructs, only PKG$^{78\text{-}355}$ yielded diffraction-quality crystals.

Overall Fold of PKG Iα$^{78\text{-}355}$

Crystals grew in the C2 space group with two molecules per asymmetric unit. Superimposition of Cα atoms from the two molecules sites gave an average root mean square deviation (rmsd) of 0.882. Initial phases were attained by molecular replacement using the CNB-A domain of PKA RIα (PDB ID 1RGS) as a search model. The structure was refined to 2.5 Å with working and free-R factor values of 0.22 and 0.28, respectively (Table 1). Each protein molecule in the asymmetric unit contained 278 amino acids, 1 cAMP molecule, and 2 phosphates.

The overall fold presents both cGMP-binding domains of the PKG Iα regulatory domain. cGMP-binding site A (residues 87–210) begins following a loop in the "hinge region," for which we see clear backbone density, followed by cGMP-binding site B (residues 211–327) and a new helical subdomain we have termed switch helix (SW, residues 328–355) (Figure 1B; see Figure S1A, secondary structural elements, available online). Both cGMP-binding sites exhibit classic features of the conserved CNB fold (Figure 2A). A rigid eight-stranded β-barrel sandwiches the phosphate binding cassette (PBC) between β strands 6 and 7 which serves as a docking site for cNTs. The β-barrel itself is flanked at the N terminus by the αN helix, the 3_{10} loop, and the αA helix (collectively termed the N3A motif) and C-terminally by the αB/αC helix. Surprisingly, the two CNB domains presented in this structure have been captured in different conformational states as is evident when comparing helical elements between A- and B-domains (Figure 2B). Superimposition of the two cGMP-binding yields an rmsd of 1.124. While the β-barrels superimpose well, there is variance in the helical subdomains.

Table 1. Data Collection and Refinement Statistics

	PKG Iα$^{78-355}$
Data collection	
Space group	C2
Cell dimensions (Å)	
A	180.2
B	66.0
C	81.6
β (°)	113.8
No. of molecule per asymmetrical unit	2
Resolution (Å)	2.50
R_{merge}	0.085 (0.52)
Completeness (%)	97.9 (93.5)
I/sigma	18.7 (1.9)
No. reflections	32166
Refinement	
Resolution (Å)	50.0–2.50
R_{work}/R_{free} (%)	22.1/27.7
No. of protein residues	556
No. of ligands/ions	4
No. of water molecules	207
Rmsd	
Bond lengths (Å)	0.008
Bond angles (°)	1.4
Ramachandran angles (%)	
Most favored	83.3
Disallowed	None

Values in parentheses are for highest-resolution shell.

The two cGMP-binding sites are separated by an elongated B/C helix at the end of the A-domain (Figure 2A). This creates a dumbbell-like topology between the two CNB domains and resembles the conformation adopted by regulatory subunits of PKA when bound to the catalytic subunits in the holoenzyme conformation (Kim et al., 2007; Wu et al., 2007). A kink in the C helix in the middle of this cleft is a likely point at which the two CNB domains undergo cGMP-mediated structural rearrangements. Residues in this kink are clearly solvent exposed (Figure 1B; Figure S1A) and proteolysis at Arg^{202} readily occurs in the absence of cGMP (Chu et al., 1997; Scholten et al., 2007). Incubation with cGMP induces conformational changes that prevent such proteolysis. Furthermore, cGMP binding increases solvent protection in this region (Alverdi et al., 2008) further suggesting that the A-domain C helix may be the center of cGMP-induced conformational changes in the regulatory domain.

The extended conformation of PKG$^{78-355}$ does not appear to allow direct communication between the A- and B-domains. This suggests that the structural determinants mediating cooperative binding of cGMP are not contributed by the core of the regulatory domain. In support of this finding, previous studies have demonstrated a loss of cooperativity upon deletion of regions outside the cGMP-binding domains (Dostmann et al., 1996; Heil et al., 1987). Moreover, in PKA holoenzyme structures of both type Iα (Kim et al., 2007) and IIα (Wu et al., 2007) the catalytic subunit docks to the cleft created by the extended topology of the CNB domains in the regulatory subunits. Residue Gln^{78}, just C-terminal to the AI domain in PKG, is positioned in the center of the two cGMP-binding sites (Figure 1B), which is where the N terminus of PKG interacts with the catalytic core of the enzyme via the AI domain (Heil et al., 1987; Hofmann et al., 2009). While the precise docking mechanism may differ in the PKG holoenzyme, the catalytic domain is likely to sit in this cleft and participate in crosstalk between the two cGMP-binding sites similar to the architectural arrangements observed in PKA.

The A-Domain Is cAMP Bound

The docking of cNTs to a CNB domain is made possible by the conserved and mobile motif of the PBC (Figure 3A) (Diller et al., 2001; McKay et al., 1982; Su et al., 1995). This short, 14 residue helix-turn contains residues that coordinate the ribose-phosphate moiety and allows for the preferential binding of cAMP versus cGMP. Invariantly, all CNB domains from cNT-regulated

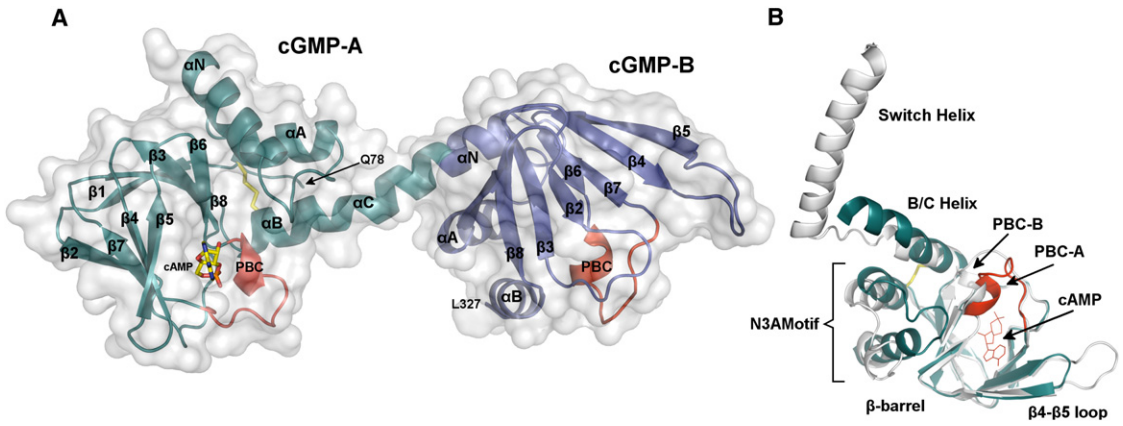

Figure 2. Topology of the cGMP-Binding Domains

(A) Overall fold of the tandem cGMP binding domains shown as cartoon representation with secondary structural elements labeled (switch helix not shown).
(B) Overlay of cGMP-A (teal) with cGMP-B (white). RMSD = 1.214 for Cα molecules. PBC from cGMP-A: red, C^{117}-C^{195} disulfide bond: yellow. See also Figure S1.

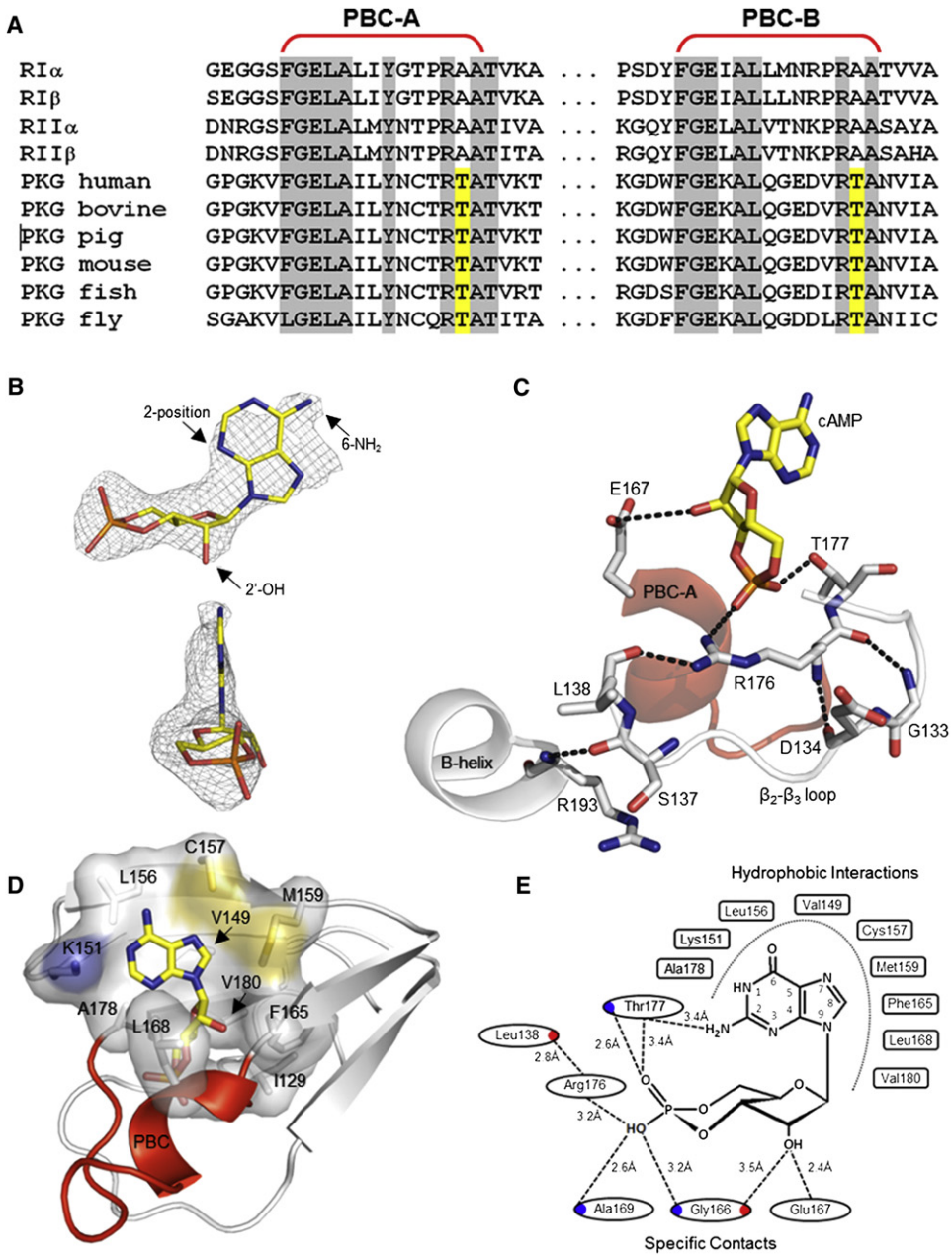

Figure 3. Features of the A-Domain

(A) Sequence alignment for PBCs from PKA and PKG Iα isoforms. Threonine residues in the 13 position of PKG PBCs are highlighted yellow.

(B) Composite omit map generated for the cNT binding sites of both A-domains contoured to 1.5 σ. *syn*-cAMP is modeled into the positive density.

(C) Specific interactions between the sugar-phosphate moiety of cAMP and residues from the PBC. The 2′-hydroxyl hydrogen bonds with Glu^{167}, the equatorial oxygen of the phosphate group interacts with Arg^{176}, and the apical oxygen contacts both the side-chain hydroxyl and backbone amino groups of Thr^{177}. The backbone carbonyl of Leu^{138} bridges communication from the guanidinium group of Arg^{176} through the β_2-β_3 loop to Arg^{193} in the B helix.

(D) A hydrophobic face accommodates the solvent-exposed nucleobase.

(E) Schematic of cNT binding to the A-domain of PKG Iα$^{78-355}$ with cGMP modeled in place of the observed cAMP. Specific hydrogen bond contacts are shown as dotted lines. Interactions coming from backbone amide (blue) and carbonyl (red) are highlighted, whereas side-chain interactions are shown from the center of the circled residue. Hydrophobic interactions with the cNT are shown as boxed residues. See also Figure S1.

protein kinases have a Glu in the 3 position and an Arg in the 12 position, which hydrogen bonds with the 2′OH and equatorial oxygen, respectively. Unique to PKG is a Thr or Ser in the 13 position of the PBC, which has been predicted to provide specificity for cGMP by providing a hydrogen bond potential with both the 2-NH_2 and apical oxygen of cGMP (Shabb and Corbin, 1992; Weber et al., 1989). PKA contains an Ala in the 13-position and mutation of this residue to a Thr produces a PKA mutant that no longer discriminates between cAMP and cGMP (Shabb et al., 1990).

To assess the occupancy of PBCs in the PKG$^{78-355}$ structure, initial phases from the molecular replacement solution were used to generate a simulated annealing composite omit map. In order to minimize model bias, side chains for the invariant Glu, Arg, and Thr residues were omitted in each PBC. A strong positive peak was observed in the A-domain which resembled a cyclic-3′,5′-nucleotide monophosphate containing a purine moiety in the *syn* configuration (Figure 3B), while the B-domain appeared cNT-free. While electron density at the 2′OH of the ribose and the 6 position of the purine was evident, we could not attribute the 6 position density to being either a keto/enol or amino group. However, there was no density extending from the 2 position where the 2-amino group of cGMP should reside. This was a clear indication that the cNT occupying the A-domain was *syn*-oriented cAMP. HPLC analysis and UV-spectroscopy confirmed the presence of cAMP and the absence of cGMP (see methods).

The primary interactions made with the cyclic nucleotide come from residues buried within the PBC. Specific contacts are made by Glu^{167}, Arg^{176}, and Thr^{177} (Figure 3C). Glu^{167} forms a hydrogen bond with the 2′OH of the ribose and Arg^{176} docks the equatorial oxygen of the phosphate. Thr^{177} hydrogen bonds with the apical oxygen of the phosphate group with both side-chain hydroxyl and backbone amino groups. Modeling of *syn*-oriented cGMP into the A-domain maintains these same contacts and shows that the 2-amino group is primed to interact with the Thr^{177} side-chain hydroxyl. The Glu and Arg contacts are similar to those used by the cAMP-PKA interaction and the previously predicted interactions with Thr^{177} are confirmed (Shabb et al., 1991; Weber et al., 1989). A schematic summary of these specific interactions with cGMP modeled into the A-domain is presented in Figure 3E.

As has been described for other CNB domain structures, cNT docking to the PBC is stabilized by a capping mechanism that sandwiches the nucleotide base between hydrophobic surface on the β-barrel, and a hydrophobic cap that moves into place upon cNT-induced structural rearrangements of the protein (Berman et al., 2005; Das et al., 2007). In the PKG$^{78-355}$ structure, the backside of the adenine ring is flanked by an array of hydrophobic contacts with no obvious hydrogen bond donor or acceptor potentials (Figures 3D). The identity of the specific capping residue is not disclosed, however, because the two CNB domains are in an extended, inactive conformation and capping occurs only after ligand-mediated conformational changes cause the two CNB domains to form a more compact structure.

A second shell of regulation is provided by the β_2-β_3 loop. In PKA this loop stabilizes the PBC arginine and provides allosteric communication of binding events in the PBC to the B helix. In the A-domain of PKG Iα, Arg^{176} is coordinated by a number of conserved residues from the β_2-β_3 loop (Figure 3C). A hydrophobic interaction is made with Ile^{130}, and the backbone carbonyl and amide of Arg^{176} forms hydrogen bonds with the Gly^{133} amide and Asp^{134} carbonyl, respectively. Furthermore, the guanidinium group of Arg^{176} interacts with the carbonyl of Leu^{138}. Communication between the β_2-β_3 loop and the B helix occurs via Arg^{193}. The backbone amide of Arg^{193} is bridged by the carbonyl of Ser^{137}. This is where PKG differs from PKA. The equivalent to Ser^{137} is Asp^{170} in the PKA RIα A-domain which hydrogen bonds not only with the backbone amide of the Arg in the B helix, but also coordinates the guanidinium of the PBC Arg. In doing so, a direct link from the PBC to the B helix hinge is made via the β_2-β_3 loop. In contrast, the PKG A-domain does not utilize this same direct allosteric mechanism. This may be a critical divergence in how these two cNT-regulated protein kinases communicate binding events in their PBCs with the rest of the molecule.

A Cys^{117}-Cys^{195} Disulfide Bond Locks A and B Helices in the A-Domain

The presence of disulfide bonds in PKG Iα have been reported and an oxidation-induced mechanism of activation has been proposed as complementary mechanism to cyclic nucleotide-mediated regulation of kinase activity (Burgoyne et al., 2007; Landgraf et al., 1991). PKG Iα contains 11 cysteine residues (Takio et al., 1984), 5 of which have been suggested to contribute to oxidation-induced activation. Cys^{42}, just C-terminal of the D/D domain forms an intermolecular disulfide bond with Cys^{42} from the opposing protomer in the holoenzyme assembly (Burgoyne et al., 2007). It has been suggested that H_2O_2-induced oxidation of PKG Iα promotes kinase activation via a bridging of these two cysteines. Additionally, exposure of PKG Iα to divalent cations with positive redox potentials promotes enzyme activation via disulfide bond formation between Cys^{117}-Cys^{195} and/or Cys^{312}-Cys^{518} (Landgraf et al., 1991). It was unclear, however, whether Cys^{117}-Cys^{195} or Cys^{312}-Cys^{518} was exclusively responsible for the observed oxidation-induced activation. Despite the observations that cysteine oxidation can lead to cGMP-independent activation of PKG Iα, no molecular mechanism of activation has been proposed.

The PKG$^{78-355}$ structure reveals a disulfide bridge between Cys^{117} in the A helix and Cys^{195} at the start of the B helix (Figure 4A). Residues immediately C-terminal of these two cysteines are solvent-exposed (Figure S1A), while a hydrophobic sheath (Phe^{80}, Ile^{114}, Ile^{191}, and Ile^{199}) surrounds the disulfide bridge and provides solvent protection (Figure 4B). In support of the oxidation-induced activation of PKG Iα previously observed (Landgraf et al., 1991), the recruitment of Phe^{80} to the hydrophobic sheath provides a hypothesis as to how the enzyme might be activated in the absence of cGMP. The capping of Cys^{117}-Cys^{195} by Phe^{80} serves to order the loop that precedes the N helix of the A-domain (Figure 4A). As the AI domain resides just adjacent to Phe^{80}, autoinhibition of the kinase may be relieved through a movement of this loop to the hydrophobic sheath. The reorganization of this region upon oxidation of Cys^{117}-Cys^{195} may disrupt the interaction between the AI and catalytic center thereby releasing the kinase from a state of autoinhibition. Furthermore, the sulfhydryl group of Cys^{312} sits on β8 of the B-domain and points inward toward the center of the β-barrel (not shown). It seems unlikely that Cys^{312} is capable of forming a disulfide bridge with Cys^{518} from the activation loop in the catalytic domain. Our structure supports the Cys^{117}-Cys^{195} disulfide bond as being involved in the metal-induced activation of PKG Iα.

Mixed Configuration of the Two CNB Domains

The cNT-dependent structural dynamics of CNB domains are well established (Berman et al., 2005; Kornev et al., 2008;

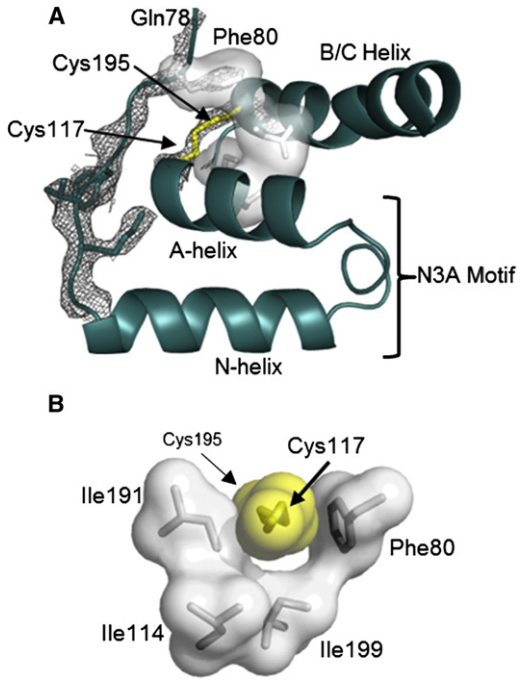

Figure 4. Details of the Cys^{117}-Cys^{195} Disulfide Bond

(A) The disulfide bridge in the A-domain between Cys^{117} and Cys^{195} (yellow) covalently links the A helix to the B helix. $2F_o$-F_c electron density contoured to 1.6σ is shown for the loop preceding the N helix and the disulfide bond.

(B) Side view of the hydrophobic sheath (gray) surrounding the disulfide bond (yellow).

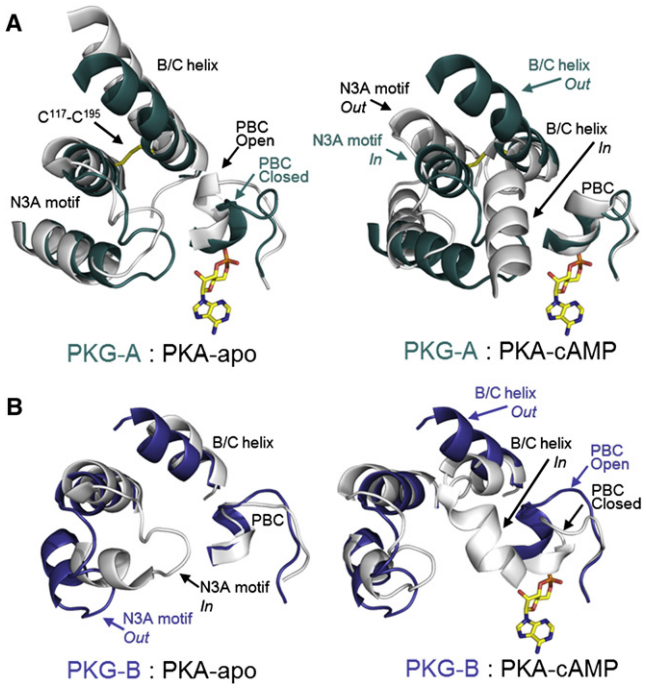

Figure 5. Comparative Overlay of Helical Subdomains for PKG and PKA CNB Domains

(A) Structural overlay of PKG A-domain (teal) with PKA A-domain (gray) from the unliganded, holoenzyme structure (left, 2QCS) and the cAMP-bound form (right, 1RGS).

(B) Structural overlay of PKG B-domain (blue) with PKA B-domain (gray) from the unliganded, holoenzyme structure (left, 2QCS) and the cAMP-bound form (right, 1RGS).

Rehmann et al., 2007). While the β-barrel does not appear to undergo significant conformational changes upon cNT binding, the α-helical subdomain moves *In* and *Out* relative to the barrel (Table 2). Ligand association with the PBC initiates these structural changes as several residues make specific interactions with the nucleotide and close the PBC. This structural change is communicated through hydrophobic residues to the N3A motif and B/C helix. As a result, an extended B/C helix forms a hinge and closes inward toward the β-barrel. This rearrangement is accompanied by an outward shift of the N3A motif. In PKA, these cNT-induced conformational changes bring the two CNB domains closer together, which is then stabilized by the association of a hydrophobic capping residue with the nucleotide base. Although there is sequence and spatial variability as to the identity of the cap that secures the nucleotide base to the β-barrel, this allosteric mechanism is present in all CNB domain structures described to date.

Table 2. Summary of the Different Positions for Each Helical Component of CNB Domains from PKA RIα and the PKG$^{78-355}$ Structure

CNB Domain	state	PBC	N3A Motif	B/C Helix
PKA RIα:Cα	apo	OPEN	IN	OUT
PKA RIα:cAMP	cNT bound	CLOSED	OUT	IN
PKG-A	Transition	CLOSED	IN	OUT
PKG-B	Transition	OPEN	OUT	OUT

The two CNB domains presented here are in a mixed, hybrid configuration, with helical elements in both apo and cNT bound orientations (Table 2). As only the high affinity A-domain is cNT bound, the A-domain PBC is closed, relative to that of the B-domain (Figure 2B). However, the subsequent conformational changes inherent to CNB domains are not observed. An overlay of the CNB domains from PKG and PKA indicate that the overall fold is conserved, but positional differences in the helical subdomain evince the hybrid nature of this PKG structure (Figures 5A and 5B). The B/C helix of the A-domain is clearly extended and the N3A motif is *In*, representative of a CNB domain in the apo, unliganded state rather than a cNT-bound conformation (Kornev et al., 2008; Figure 5A). Despite the A-domain PBC being occupied by cAMP, allosteric communication of this binding event with the rest of the domain is severed. Interestingly, the Cys^{117}-Cys^{195} disulfide bond provides a major structural determinant for this stable transition state. The covalent bridging of the A helix to the B helix prevents the B/C helix from closing upon cNT binding to the PBC. In turn, the N3A motif cannot move out from the β-barrel (Figure 5A, arrow). This disulfide bond therefore uncouples communication of allosteric events in the A-domain from being transmitted to the B-domain.

The B-domain of this PKG structure is similarly locked in a hybrid conformation. This CNB domain is cNT free, thus the unbound PBC is *Open* and maintains an extended B/C helix (Figure 5B). However, the N3A motif is also *Out*, an orientation

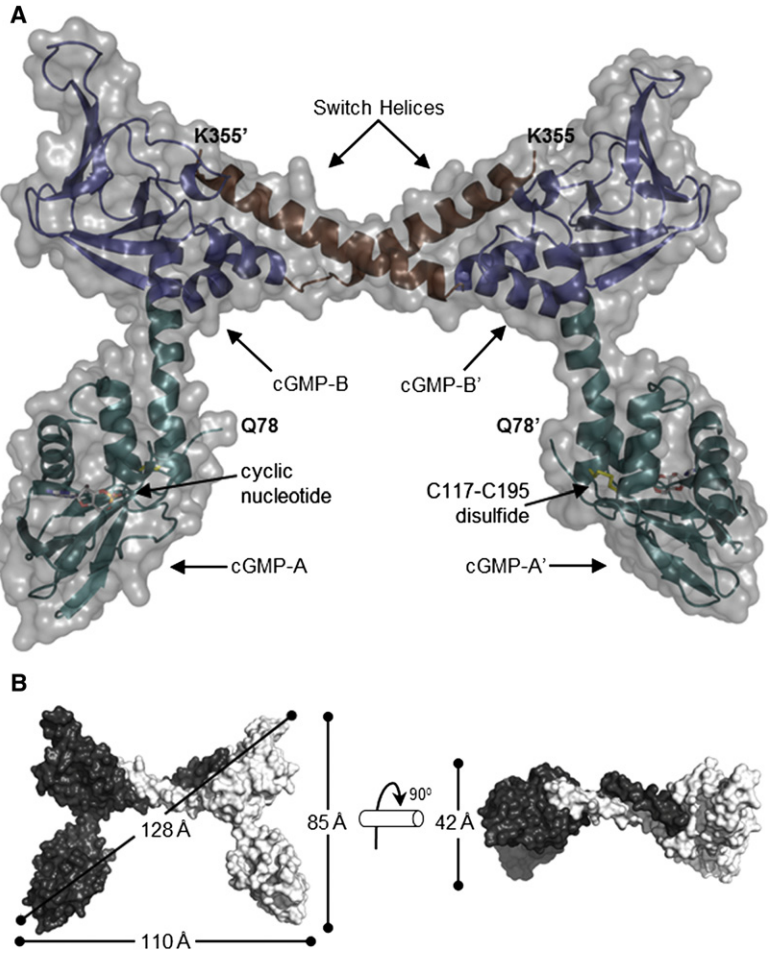

Figure 6. Dimeric View of PKG$^{78\text{-}355}$ Protomers

(A) Ribbon diagram of two PKG$^{78\text{-}355}$ protomers as observed in the asymmetric unit. Color coding is same as in Figure 2A.

(B) "Front" and Top" views of surface representation of the PKG$^{78\text{-}355}$ dimer to illustrate the crossing of switch helices. See also Figure S2.

reminiscent of a cNT-bound state (Kornev et al., 2008). The B-domain N3A motif is stabilized in the *Out* position by a set of hydrophobic residues originating from the C-terminal end of the SW in the other molecule in the asymmetric unit. The two symmetry mates are related by noncrystallographic symmetry and this interaction promotes a previously uncharacterized docking interface between PKG Iα protomers, which is described in detail below.

PKG$^{78\text{-}355}$ Protomers Interact via Their Switch Helices

Remarkably, the PKG$^{78\text{-}355}$ crystal structure forms a symmetry-related dimer through the formation of an interface between the SW and the opposing B-domain (Figures 6A and 6B). It is well established that PKG assembles into parallel homodimers, an assembly mediated by leucine zipper motifs at the immediate N termini. The structure presented here provides the first evidence for intermolecular communication at sites distal to the classical N-terminal D/D domain. The SW extends from the B-domain and residues at the C terminus of each SW interact with an open hydrophobic network in the B-domain of the opposing protomer (Figures 7A and 7B). Hydrophobic "knobs" at the end of the SW (residues 350–354) stabilize the open N3A motif in the B-domain of the neighboring protomer. Side chains from Phe^{350}, Phe^{351}, and Leu^{354} fill the void created by an extensive hydrophobic "nest" (Figures 7A and 7B). The eight residues that comprise the nest (Phe^{221}, Leu^{224}, Leu^{232}, Trp^{288}, Gln^{295}, Phe^{320}, Ile^{324}, Leu^{327}) are noncontiguous and recruited from the entire B-domain (Figure S1A). This knob-nest interface is further strengthened by Asn^{353}, the only polar residue at the end of the SW, which forms a hydrogen bond with the backbone carbonyl of Thr^{220} in the 3_{10} loop of the B-domain (Figures 7A and 7B). Formation of this dimeric assembly protects 2740 Å^2 of surface area, and has a free energy (ΔG) of 15.8 kcal/mol required for dissociation, an indication that this arrangement is thermodynamically stable in solution. Native PAGE analysis of PKG$^{78\text{-}355}$ in solution displays a small population of dimeric protein (Figure S2A). Similarly, the migration of crystalline PKG$^{78\text{-}355}$ is consistent with a dimer (Figure S2B).

Our initial DxMS studies on PKG$^{78\text{-}355}$ offered further validation of the significance of this knob-nest interface. Analysis of peptide fragments from the SW indicated that the C-terminal residues containing the hydrophobic knobs and Asn^{353} had a slower rate of deuterium exchange compared with residues in the more solvent-exposed region of this helix. This finding suggested that the very C terminus of the SW is protected in solution and that the knob-nest interaction may serve as the focal point of interchain communication between PKG protomers. Interestingly, the knob residues appear to be unique to PKG I isoforms, as PKG II has a large amino acid insertion at the site of the SW (see sequence alignment, Figure S1A). However, hydrophobic residues at the equivalent nest positions are conserved in both PKG I and II isoforms.

Mutational Disruption of the Knob-Nest Interface in Full-Length PKG Iα Decreases the Activation Constant and Suggests a Tethering Mechanism for the Catalytic Domain

The functional relevance of the knob-nest interface was probed by Alanine scanning mutagenesis of the SW knob residues in full-length PKG Iα containing both the N-terminal D/D and the catalytic domains. Extracts from HEK293 cells expressing wild-type and mutant PKG Iα were examined for phosphoryl transfer activity. Removal of the specific hydrogen bond provided by Asn^{353} (N^{353}A) resulted in a significantly decreased activation constant (Figure 7C and Table 3). The entire knob-nest interface was disrupted by a quadruple mutation wherein all hydrophobic knob residues in addition to the specific

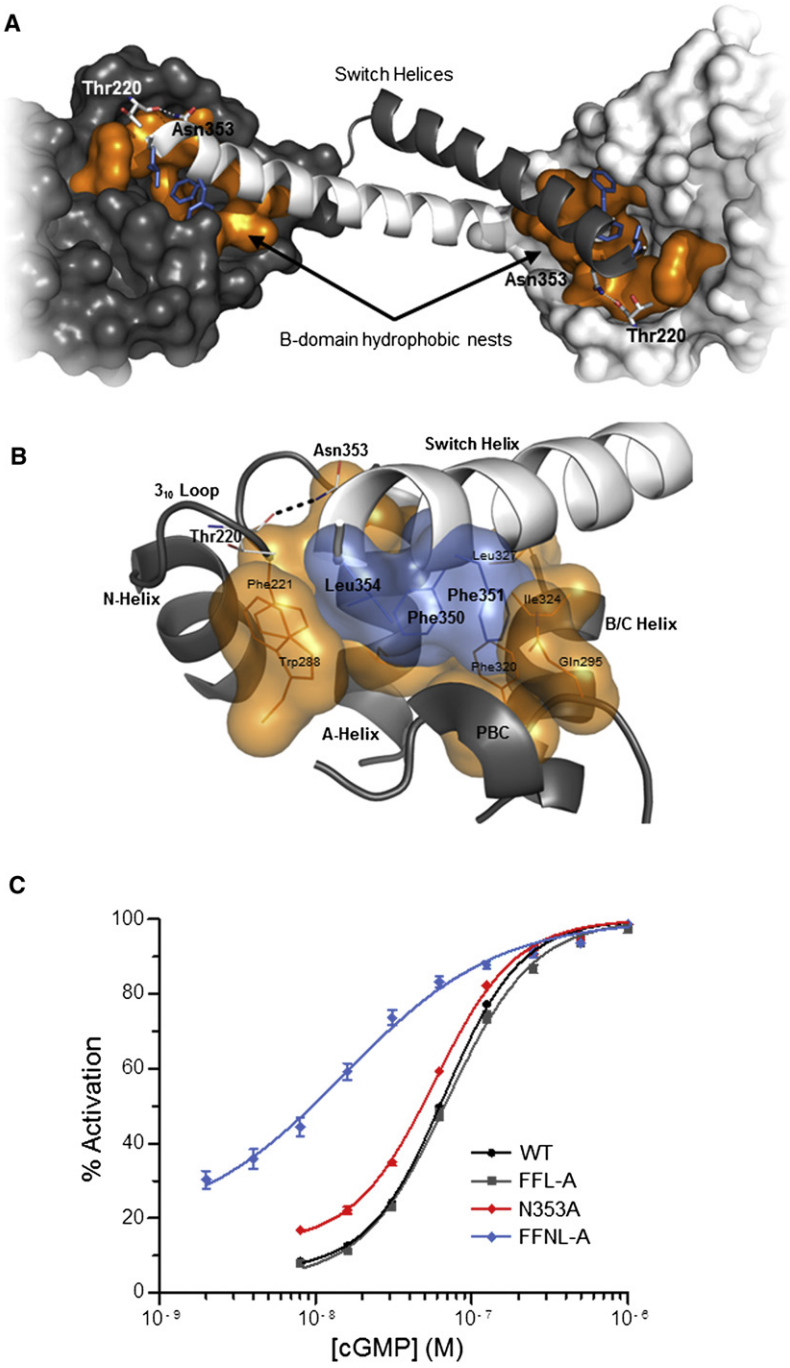

Figure 7. Structural Details of the Switch Helix-Mediated Dimer Interface

(A) "Top" view of switch helices (SW) and their assemblage with the neighboring B-domain: hydrophobic knobs at the end of the SW (blue), residues that comprise a hydrophobic nest in the B-domain (orange).

(B) Details of the knob-nest assembly that mediates PKG^{78-355} dimerization. The switch helix (white), and helical features from the neighboring B-domain (gray) are represented as ribbons.

(C) Kinetic Analysis of WT PKG Iα (black) and SW knob mutants $F^{350}A$, $F^{351}A$, $L^{354}A$ (gray), $N^{353}A$ (red), and $F^{350}A$, $F^{351}A$, $N^{353}A$, $L^{354}A$ (blue). See also Figures S1 and S2.

Asn^{353} were substituted for alanine ($F^{350}A$, $F^{351}A$, $N^{353}A$, $L^{354}A$). Neutralization of these interactions further reduced the activation constant greater than 4-fold (Figure 7C and Table 3). Additionally, this mutant displayed a loss of cooperativity (n_H). While we were unable to calculate absolute basal and V_{max} values, the relative changes in K_A, combined with the observed decrease in Hill coefficient, illustrates the importance of the knob-nest interface in maintaining the kinetic fidelity of PKG Iα. In the context of full-length PKG Iα, the SW seems to act as a tether for the catalytic domain, disruption of which causes the kinase to be more easily activated.

Direct communication between regulatory and catalytic elements is not without precedent in AGC kinases. In PKA, there are at least four major sites of contact between the R and C subunits, with CNB domain A providing the largest docking surface for the C subunit (Boettcher et al., 2011; Kim et al., 2007). Likewise, in PKC βII, the conserved NFD motif in the catalytic domain is clamped by the diacylglycerol-binding C1B domain until fully activated (Leonard et al., 2011). While these interactions highlight the diversity of interdomain complementarity among AGC kinase family members, they also demonstrate clear commonalities in their mechanisms of regulation.

This crystal structure provides the first atomic view of PKG and provides a new platform for understanding the allosteric regulation of the holoenzyme complex. The overall fold of PKG^{78-355} is surprising, in that a previously uncharacterized allosteric interface promotes a novel means of communication between PKG^{78-355} protomers wherein the catalytic domain can be tethered between inactive and active states. The crossing of switch helices between protomers (Figure 6B) suggests that the catalytic domain from one protomer is regulated in part by the regulatory domain of the other protomer. A complete understanding of PKG structural dynamics will undoubtedly require additional studies, however this new structure presents crucial details into the long sought after mechanism of allosteric PKG activation.

EXPERIMENTAL PROCEDURES

Bacterial Protein Expression and Purification

DNA for bovine PKG Iα encoding amino acids Q^{78}-K^{355} was amplified by PCR using the primers 5′-CGGGATCCATGCAGGCATTCCGGAAGTTC-3′ (sense) and 5′-GGAATTCCTACTACTTCAGGTTGGCGAAG-3′ (antisense). The PCR product was digested with BamHI and EcoRI and ligated into pRSET-A

Table 3. Summary of Kinetic Analysis from Figure 7C

Mutation	K_A (nM)	n_H	Fold Activation
WT (n = 12)	67 ± 2	1.7 ± 0.09	11.0
$F^{350}A/F^{351}A/L^{354}A$ (n = 4)	70 ± 5	1.6 ± 0.06	12.3
$N^{353}A$ (n = 9)	57 ± 1	1.7 ± 0.06	5.9
$F^{350}A/F^{351}A/N^{353}A/L^{354}A$ (n = 10)	15.3 ± 1.7	0.8 ± 0.09	3.1

Activation constants (K_A) and Hill coefficients (n_H) are presented for WT PKG Iα and SW knob mutants. A statistically significant difference in K_A was noted for both the $N^{353}A$ and $F^{350}A/F^{351}A/N^{353}A/L^{354}A$ mutants ($p < 0.001$) compared with WT PKG Iα.

(Invitrogen) in frame with the N-terminal 6x-His tag. The plasmid was transformed into *E. coli* BL21 and 5 ml starter cultures in LB were allowed to grow to OD_{600} = 0.6 at 37°C, 300 RPM in the presence of 50 μg/ml Ampicillin. One liter of Overnight Express (Novagen) media was inoculated 1:1000 in 4 liter baffled flasks with the mid-log starter prep and grown at 25°C, 300 RPM for 16–24 hr. Bacteria were harvested by centrifugation at 5K RPM for 10 min at 4°C, and pellets were stored at −80°C. Pellets were resuspended in 5 ml/gram of 50 mM MES (pH 6.8), 100 mM NaCl, 5 mM $MgCl_2$, 3 mM TCEP, 5% glycerol (Buffer A) plus protease inhibitors. Cells were lysed at 1200 psi using a french pressure cell. Homogenates were clarified via centrifugation at 15K RPM for 90 min at 4°C and recombinant PKG $I\alpha^{78\text{-}355}$ was purified from the supernatants on a Profinia protein purification system (Biorad) using the native IMAC protocol. Eluted protein was subjected to three rounds of dialysis in 2 liters of buffer A at 4°C. A secondary purification step was performed on an AKTAprime FPLC system by passing Ni^{2+}-purified protein over a HiLoad 16/60 Superdex 75 (GE Healthcare) gel filtration column and collecting 1 ml fractions in Buffer A. Protein homogeneity was assessed via SDS-PAGE and Coomassie staining. Desired fractions were pooled and concentrated using 10K MWCO centrifugal concentrators (Sartorius). Typical yields were 100 mg purified protein per liter of media.

Crystallization, Data Collection, and Model Refinement

Sparse matrix kits from Hampton Research were used to screen initial crystal growth conditions. Crystals used for data collection were grown via hanging drop vapor diffusion in 2.2 M $(NH_4)_2SO_4$, 100 mM Tris (pH 8.0), 0.2% MPD at a protein concentration of 25–35 mg/ml at 20°C. Crystals were cryoprotected for 10–30 min in 2 M Li_2SO_4, 100 mM Tris (pH 8.0), 0.2% MPD and flash frozen in liquid N_2. 2.5 Å diffraction data were collected at beamline 8.2.1 at the Advanced Light Source, Lawrence Berkeley National Laboratory. HKL2000 was used for data processing and scaling (Minor, 1997). Phases were generated with the program Phaser (McCoy et al., 2007) using the PKA regulatory domain (PDB ID 1RGS) as a search model. Crystals grew in the C2 space group with two molecules per asymmetric unit. The PKG $I\alpha^{78\text{-}355}$ model was manually built into electron density using the programs TURBO-FRODO (Roussel and Cambillau, 1991) and Coot (Emsley et al., 2010). CNS (Brünger et al., 1998) was used for structure refinement. Publication-quality images were generated using Pymol (The PyMOL Molecular Graphics System, Version 1.2r3pre, Schrödinger, LLC). Interface and assembly measurements of symmetry mates were calculated using the protein interfaces, surfaces, and assemblies service PISA at European Bioinformatics Institute (Krissinel and Henrick, 2007).

Deuterium on Exchange

All deuterium exchange reactions were performed on ice, in a 4°C cold room. Exchange reactions were initiated by adding 6 μl buffered D_2O to 2 μl purified PKG $I\alpha^{78\text{-}355}$ at 7 mg/ml. At the appropriate time points exchange was quenched by adding 12 μl 1.6 M GuHCl, 0.8% formic acid. In addition, nondeuterated samples were prepared by incubating the protein in buffered H_2O. Fully deuterated samples were prepared by incubating the protein in D_20 buffer containing 1% formic acid overnight at room temperature. The samples were frozen on dry ice and stored at −80°C until analysis by mass spectrometry. Samples were manually thawed on wet ice and immediately analyzed by LC-MS. Procedures for pepsin digestion for DXMS have been described previously (Burns-Hamuro et al., 2005; Hamuro et al., 2004; Pantazatos et al., 2004; Spraggon et al., 2004). Briefly, the samples were passed through an immobilized pepsin column and the protease-generated peptides were collected on a C18 HPLC column. The peptides were eluted from the C18 column and the effluent was directed to a Thermo Finnigan LCQ electrospray ion trap type mass spectrometer with data acquisition in either MS1 profile mode or data-dependent MS2 mode. The pepsin-generated peptides from the MS/MS data sets were identified using SEQUEST (Thermo Finnigan Inc.), followed by analysis using customized DXMS data reduction software (Sierra Analytics Inc., Modesto, CA). Corrections for back exchange were made through measurement of loss of deuterium from fully deuterated samples. Deuterium incorporation for each peptide was calculated using the methods of Zhang and Smith (1993):

$$\textit{deuteration level}\ (\%) = \frac{m(p) - m(N)}{m(F) - m(N)} \times 100,$$

where $m(P)$, $m(N)$, and $m(F)$ are the centroid value of the partially deuterated, nondeuterated, and fully deuterated peptide, respectively. The experiments were performed twice, and the reported results are the average of the two experiments.

Cyclic Nucleotide Analysis

To confirm the copurification of cAMP, purified $PKG^{78\text{-}355}$ was incubated on ice in a 1:1 ratio of acetonitrile. The extract was clarified via centrifugation at 4°C and the supernatant was subjected to UV-spectroscopy. The extract had a single peak with a λ_{max} of 258 nm and lacked the characteristic cGMP shoulder. The same extract was subjected to HPLC analysis using a Merck Hitachi HPLC system comprising a L-2130 pump, a L-2400 UV detector, a L-2350 column oven, and a L-2200 autosampler, and data were processed with EZChrom Elite evaluation software (3.2.1). Isocratic runs were performed at 30°C on a RP-18 reversed phase silica column (250 × 4 mm, ODS A,YMC) with 2.5% isopropanol and 25 mM triethylammonium formate buffer (pH 6.9) with a flow of 1 ml/min at 255 nm.

Mammalian Protein Expression

WT PKG Iα was cloned into pcDNA 3.1 using BamHI and EcoRI. Mutations were made using QuickChange site-directed mutagenesis (Agilent Technologies, Santa Clara, CA) per manufacturer's recommendations. HEK293 cells grown in 10 cm dishes were transfected for 5 hr using Metafectene (Biontex, San Diego, CA) at a ratio of 20 μg DNA per 60 μl lipid. Sixty hours after transfection cells were harvested by scraping into PBS, 2 mM benzamidine-HCl, 200 μM EDTA. Protein concentration was determined by the Bradford method and stocks were stored in 50% glycerol at −20°C.

Kinetic Analysis

Determination of activation constants was performed using a [γ-^{32}P]-ATP transfer assay as previously reported (Ruth et al., 1991; Tegge et al., 1995). Briefly, 0.5 μg of wild-type or mutant protein from PKG-transfected HEK293 cells was incubated in buffer with various concentration of cGMP in the presence of [γ-^{32}P]-ATP and the PKG-specific peptide substrate TQAKRKK SLAMA (Dostmann et al., 1999). Aliquots, spotted on P81 Whatman paper were subjected to scintillation counting. All experiments were performed in the presence of the PKA-specific inhibitor, $PKI^{5\text{-}24}$ (70 nM) to suppress endogenous PKA activity. Mock-transfected cells did not show any activity.

ACCESSION NUMBERS

Coordinates have been deposited in the Protein Data Bank with accession code 3SHR.

SUPPLEMENTAL INFORMATION

Supplemental Information includes two figures and can be found with this article online at doi:10.1016/j.str.2011.06.012.

ACKNOWLEDGMENTS

We thank Nico Villanueva, Karl Zahn, and Brian Eckenroth of the UVM Center for X-ray Crystallography for their expertise. HPLC analysis was graciously performed by Hans-G. Genieser and Frank Schwede of BIOLOG Life Science Institute, Bremen, Germany. This work was supported by NIH grants HL68891 (B.W.O., C.J.M., C.K.N., W.R.D.), GM34921 (J.W., A.P.K., S.S.T.), CA099835, CA118595, AI076961, AI081982, AI2008031, GM020501, GM066170, NS070899, GM093325, and RR029388 (V.L.W.), CA124517 (D.E.C.), and by the Totman Trust for Medical Research (C.K.N., W.R.D.).

Received: February 14, 2011
Revised: June 8, 2011
Accepted: June 13, 2011
Published: September 6, 2011

REFERENCES

Aitken, A., Hemmings, B.A., and Hofmann, F. (1984). Identification of the residues on cyclic GMP-dependent protein kinase that are autophosphorylated in the presence of cyclic AMP and cyclic GMP. Biochim. Biophys. Acta *790*, 219–225.

Alverdi, V., Mazon, H., Versluis, C., Hemrika, W., Esposito, G., van den Heuvel, R., Scholten, A., and Heck, A.J. (2008). cGMP-binding prepares PKG for substrate binding by disclosing the C-terminal domain. J. Mol. Biol. *375*, 1380–1393.

Berman, H.M., Ten Eyck, L.F., Goodsell, D.S., Haste, N.M., Kornev, A., and Taylor, S.S. (2005). The cAMP binding domain: an ancient signaling module. Proc. Natl. Acad. Sci. USA *102*, 45–50.

Boettcher, A.J., Wu, J., Kim, C., Yang, J., Bruystens, J., Cheung, N., Pennypacker, J.K., Blumenthal, D.A., Kornev, A.P., and Taylor, S.S. (2011). Realizing the allosteric potential of the tetrameric protein kinase A RIα holoenzyme. Structure *19*, 265–276.

Brünger, A.T., Adams, P.D., Clore, G.M., DeLano, W.L., Gros, P., Grosse-Kunstleve, R.W., Jiang, J.S., Kuszewski, J., Nilges, M., Pannu, N.S., et al. (1998). Crystallography & NMR system: A new software suite for macromolecular structure determination. Acta Crystallogr. D Biol. Crystallogr. *54*, 905–921.

Burgoyne, J.R., Madhani, M., Cuello, F., Charles, R.L., Brennan, J.P., Schröder, E., Browning, D.D., and Eaton, P. (2007). Cysteine redox sensor in PKGIa enables oxidant-induced activation. Science *317*, 1393–1397.

Burns-Hamuro, L.L., Hamuro, Y., Kim, J.S., Sigala, P., Fayos, R., Stranz, D.D., Jennings, P.A., Taylor, S.S., and Woods, V.L., Jr. (2005). Distinct interaction modes of an AKAP bound to two regulatory subunit isoforms of protein kinase A revealed by amide hydrogen/deuterium exchange. Protein Sci. *14*, 2982–2992.

Chu, D.M., Corbin, J.D., Grimes, K.A., and Francis, S.H. (1997). Activation by cyclic GMP binding causes an apparent conformational change in cGMP-dependent protein kinase. J. Biol. Chem. *272*, 31922–31928.

Das, R., Esposito, V., Abu-Abed, M., Anand, G.S., Taylor, S.S., and Melacini, G. (2007). cAMP activation of PKA defines an ancient signaling mechanism. Proc. Natl. Acad. Sci. USA *104*, 93–98.

Diller, T.C., Madhusudan, Xuong, N.H., and Taylor, S.S. (2001). Molecular basis for regulatory subunit diversity in cAMP-dependent protein kinase: crystal structure of the type II beta regulatory subunit. Structure *9*, 73–82.

Dostmann, W.R., Koep, N., and Endres, R. (1996). The catalytic domain of the cGMP-dependent protein kinase Ialpha modulates the cGMP-binding characteristics of its regulatory domain. FEBS Lett. *398*, 206–210.

Dostmann, W.R., Nickl, C., Thiel, S., Tsigelny, I., Frank, R., and Tegge, W.J. (1999). Delineation of selective cyclic GMP-dependent protein kinase Ialpha substrate and inhibitor peptides based on combinatorial peptide libraries on paper. Pharmacol. Ther. *82*, 373–387.

Emsley, P., Lohkamp, B., Scott, W.G., and Cowtan, K. (2010). Features and development of Coot. Acta Crystallogr. D Biol. Crystallogr. *66*, 486–501.

Feil, R., Bigl, M., Ruth, P., and Hofmann, F. (1993). Expression of cGMP-dependent protein kinase in Escherichia coli. Mol. Cell. Biochem. *127-128*, 71–80.

Francis, S.H., and Corbin, J.D. (1994). Structure and function of cyclic nucleotide-dependent protein kinases. Annu. Rev. Physiol. *56*, 237–272.

Francis, S.H., Poteet-Smith, C., Busch, J.L., Richie-Jannetta, R., and Corbin, J.D. (2002). Mechanisms of autoinhibition in cyclic nucleotide-dependent protein kinases. Front. Biosci. *7*, d580–d592.

Gill, G.N., and Garren, L.D. (1971). Role of the receptor in the mechanism of action of adenosine 3′:5′-cyclic monophosphate. Proc. Natl. Acad. Sci. USA *68*, 786–790.

Gill, G.N., Walton, G.M., and Sperry, P.J. (1977). Guanosine 3′:5′-monophosphate-dependent protein kinase from bovine lung. Subunit structure and characterization of the purified enzyme. J. Biol. Chem. *252*, 6443–6449.

Hamuro, Y., Anand, G.S., Kim, J.S., Juliano, C., Stranz, D.D., Taylor, S.S., and Woods, V.L., Jr. (2004). Mapping intersubunit interactions of the regulatory subunit (Rlalpha) in the type I holoenzyme of protein kinase A by amide hydrogen/deuterium exchange mass spectrometry (DXMS). J. Mol. Biol. *340*, 1185–1196.

Heil, W.G., Landgraf, W., and Hofmann, F. (1987). A catalytically active fragment of cGMP-dependent protein kinase. Occupation of its cGMP-binding sites does not affect its phosphotransferase activity. Eur. J. Biochem. *168*, 117–121.

Hofmann, F., Bernhard, D., Lukowski, R., and Weinmeister, P. (2009). cGMP regulated protein kinases (cGK). Handb Exp Pharmacol, 137–162.

Kennelly, P.J., and Krebs, E.G. (1991). Consensus sequences as substrate specificity determinants for protein kinases and protein phosphatases. J. Biol. Chem. *266*, 15555–15558.

Kim, C., Cheng, C.Y., Saldanha, S.A., and Taylor, S.S. (2007). PKA-I holoenzyme structure reveals a mechanism for cAMP-dependent activation. Cell *130*, 1032–1043.

Kornev, A.P., Taylor, S.S., and Ten Eyck, L.F. (2008). A generalized allosteric mechanism for cis-regulated cyclic nucleotide binding domains. PLoS Comput. Biol. *4*, e1000056.

Krissinel, E., and Henrick, K. (2007). Inference of macromolecular assemblies from crystalline state. J. Mol. Biol. *372*, 774–797.

Landgraf, W., and Hofmann, F. (1989). The amino terminus regulates binding to and activation of cGMP-dependent protein kinase. Eur. J. Biochem. *181*, 643–650.

Landgraf, W., Regulla, S., Meyer, H.E., and Hofmann, F. (1991). Oxidation of cysteines activates cGMP-dependent protein kinase. J. Biol. Chem. *266*, 16305–16311.

Leonard, T.A., Różycki, B., Saidi, L.F., Hummer, G., and Hurley, J.H. (2011). Crystal structure and allosteric activation of protein kinase C βII. Cell *144*, 55–66.

McCoy, A.J., Grosse-Kunstleve, R.W., Adams, P.D., Winn, M.D., Storoni, L.C., and Read, R.J. (2007). Phaser crystallographic software. J. Appl. Cryst. *40*, 658–674.

McKay, D.B., Weber, I.T., and Steitz, T.A. (1982). Structure of catabolite gene activator protein at 2.9-A resolution. Incorporation of amino acid sequence and interactions with cyclic AMP. J. Biol. Chem. *257*, 9518–9524.

Minor, Z.O.W., ed. (1997). Processing of X-ray Diffraction Data Collected in Oscillation Mode, part A edn (New York: Academic Press).

Pantazatos, D., Kim, J.S., Klock, H.E., Stevens, R.C., Wilson, I.A., Lesley, S.A., and Woods, V.L., Jr. (2004). Rapid refinement of crystallographic protein construct definition employing enhanced hydrogen/deuterium exchange MS. Proc. Natl. Acad. Sci. USA *101*, 751–756.

Pfeifer, A., Ruth, P., Dostmann, W., Sausbier, M., Klatt, P., and Hofmann, F. (1999). Structure and function of cGMP-dependent protein kinases. Rev. Physiol. Biochem. Pharmacol. *135*, 105–149.

Reed, R.B., Sandberg, M., Jahnsen, T., Lohmann, S.M., Francis, S.H., and Corbin, J.D. (1996). Fast and slow cyclic nucleotide-dissociation sites in cAMP-dependent protein kinase are transposed in type Ibeta cGMP-dependent protein kinase. J. Biol. Chem. *271*, 17570–17575.

Rehmann, H., Wittinghofer, A., and Bos, J.L. (2007). Capturing cyclic nucleotides in action: snapshots from crystallographic studies. Nat. Rev. Mol. Cell Biol. *8*, 63–73.

Richie-Jannetta, R., Busch, J.L., Higgins, K.A., Corbin, J.D., and Francis, S.H. (2006). Isolated regulatory domains of cGMP-dependent protein kinase Ialpha and Ibeta retain dimerization and native cGMP-binding properties and undergo isoform-specific conformational changes. J. Biol. Chem. *281*, 6977–6984.

Roussel, A., and Cambillau, C. (1991). Silicon Graphics, Inc (CA: Mountain View).

Ruth, P., Landgraf, W., Keilbach, A., May, B., Egleme, C., and Hofmann, F. (1991). The activation of expressed cGMP-dependent protein kinase isozymes I alpha and I beta is determined by the different amino-termini. Eur. J. Biochem. *202*, 1339–1344.

Sandberg, M., Natarajan, V., Ronander, I., Kalderon, D., Walter, U., Lohmann, S.M., and Jahnsen, T. (1989). Molecular cloning and predicted full-length amino acid sequence of the type I beta isozyme of cGMP-dependent protein kinase from human placenta. Tissue distribution and developmental changes in rat. FEBS Lett. *255*, 321–329.

Scholten, A., Fuss, H., Heck, A.J., and Dostmann, W.R. (2007). The hinge region operates as a stability switch in cGMP-dependent protein kinase I alpha. FEBS J. *274*, 2274–2286.

Shabb, J.B., Buzzeo, B.D., Ng, L., and Corbin, J.D. (1991). Mutating protein kinase cAMP-binding sites into cGMP-binding sites. Mechanism of cGMP selectivity. J. Biol. Chem. *266*, 24320–24326.

Shabb, J.B., and Corbin, J.D. (1992). Cyclic nucleotide-binding domains in proteins having diverse functions. J. Biol. Chem. *267*, 5723–5726.

Shabb, J.B., Ng, L., and Corbin, J.D. (1990). One amino acid change produces a high affinity cGMP-binding site in cAMP-dependent protein kinase. J. Biol. Chem. *265*, 16031–16034.

Spraggon, G., Pantazatos, D., Klock, H.E., Wilson, I.A., Woods, V.L., Jr., and Lesley, S.A. (2004). On the use of DXMS to produce more crystallizable proteins: structures of the T. maritima proteins TM0160 and TM1171. Protein Sci. *13*, 3187–3199.

Su, Y., Dostmann, W.R., Herberg, F.W., Durick, K., Xuong, N.H., Ten Eyck, L., Taylor, S.S., and Varughese, K.I. (1995). Regulatory subunit of protein kinase A: structure of deletion mutant with cAMP binding domains. Science *269*, 807–813.

Takio, K., Wade, R.D., Smith, S.B., Krebs, E.G., Walsh, K.A., and Titani, K. (1984). Guanosine cyclic 3′,5′-phosphate dependent protein kinase, a chimeric protein homologous with two separate protein families. Biochemistry *23*, 4207–4218.

Tegge, W., Frank, R., Hofmann, F., and Dostmann, W.R. (1995). Determination of cyclic nucleotide-dependent protein kinase substrate specificity by the use of peptide libraries on cellulose paper. Biochemistry *34*, 10569–10577.

Vaandrager, A.B., Hogema, B.M., and de Jonge, H.R. (2005). Molecular properties and biological functions of cGMP-dependent protein kinase II. Front. Biosci. *10*, 2150–2164.

Weber, I.T., Shabb, J.B., and Corbin, J.D. (1989). Predicted structures of the cGMP binding domains of the cGMP-dependent protein kinase: a key alanine/threonine difference in evolutionary divergence of cAMP and cGMP binding sites. Biochemistry *28*, 6122–6127.

Wernet, W., Flockerzi, V., and Hofmann, F. (1989). The cDNA of the two isoforms of bovine cGMP-dependent protein kinase. FEBS Lett. *251*, 191–196.

Wolfe, L., Francis, S.H., and Corbin, J.D. (1989). Properties of a cGMP-dependent monomeric protein kinase from bovine aorta. J. Biol. Chem. *264*, 4157–4162.

Wu, J., Brown, S.H., von Daake, S., and Taylor, S.S. (2007). PKA type IIalpha holoenzyme reveals a combinatorial strategy for isoform diversity. Science *318*, 274–279.

Zhang, Z., and Smith, D.L. (1993). Determination of amide hydrogen exchange by mass spectrometry: a new tool for protein structure elucidation. Protein Sci. *2*, 522–531.

Zhao, J., Trewhella, J., Corbin, J., Francis, S., Mitchell, R., Brushia, R., and Walsh, D. (1997). Progressive cyclic nucleotide-induced conformational changes in the cGMP-dependent protein kinase studied by small angle X-ray scattering in solution. J. Biol. Chem. *272*, 31929–31936.

Note Added in Proof

Subsequent to our initial submission of this manuscript, Kim, et al., PLoS One. 2011 Apr 19;6(4):e18413, published a structure describing the cGMP binding site A, the details of which support our structural findings.